ICIC Express Letters
Part B: Applications
Volume **7**, Number **8**, August **2016**

ICIC International ©2016 ISSN 2185-2766
pp. **1693–1698**

AN OPTIMIZED PID MAGNETIC BEARING CONTROL SYSTEM BASED ON PARTICLE SWARM OPTIMIZATION

Chin-Tsung Hsieh, Her-Terng Yau*, Jia-Shou Zheng
Cheng-Chi Wang and Hong-Cheng Chen

Department of Electrical Engineering
National Chin-Yi University of Technology
No. 57, Sec. 2, Zhongshan Rd., Taiping Dist., Taichung 41170, Taiwan
*Corresponding author: htyau@ncut.edu.tw

Received February 2016; accepted May 2016

Abstract. *This paper describes a study of optimized Proportion-Integral-Differential (PID) control for a magnetic bearing system. Such a system is nonlinear and extremely unstable and this poses the extremely important question of how to perform modeling and control. In this study curve fitting was used to construct a dynamic equation model. The model was built and verified in practical experiments and found to be of relatively high accuracy. Particle Swarm Optimization (PSO) was used to search for optimizing PID control parameters so that MATLAB software could be used in conjunction with the dSPACE hardware to develop a control platform. Practical experiments verified that the parameters obtained using the PSO algorithm, could be used to directly control the system to reach a desired position, and this method was more efficient than the trial-and-error manual adjustment of PID control parameters.*
Keywords: Magnetic bearing, PID, Particle Swarm Optimization

1. **Introduction.** Magnetic levitation refers to electromagnetic levitation (EML) technology where the primary concept is the application of a high frequency electromagnetic field to a metal to generate eddy currents on the surface. These eddy currents generate an opposing, or repelling force, that in one popular demonstration, will suspend a metal ball in the air. There are three variations of levitation technique currently in use around the world; these include the Japanese superconducting electromagnetic levitation system, the German constant conducting electromagnetic system and the permanent magnet levitation used in China. The assembly structure in these magnetic levitation systems almost always includes a substantial number of nonlinear elements, and so complicated nonlinear magnetic phenomena are inevitable. Theoretically the inductance of an electromagnet that uses highly conductive magnetic material and solenoid coils is a constant value. However, small variations in the distance between the electromagnet and the ferromagnetic substance will cause nonlinear changes of inductance and so the electromagnets are always nonlinear elements in any electromagnetic levitation system.

Currently, electromagnetic levitation is being widely applied in a number of fields, such as magnetic bearings [1], the magnetic levitation of railway trains [2], and the vibration interference isolation of sensing elements and instrument tables [3], among which the magnetic bearing system is the most well-known. However, because a magnetic bearing system is extremely unstable and nonlinear, the question of how to stabilize the system and hold a desired position using a controller is a significant issue. Some recent controller designs include: variable structure control [4], PID control [5], sliding mode control [6] and so on. However, an electromagnetic levitation system cannot be as easily controlled by a PID controller as a conventional linear system and it is extremely difficult to use the trial-and-error method manually to adjust the control parameters and arrive at a

satisfactory outcome. Therefore, an intelligent PSO algorithm is used in this study to find optimized Proportion-Integral-Differential (PID) control parameters. This method does not require complex control theory and it can be easier and faster to find the optimal solution.

In Section 2 of this paper, an actual magnetic bearing system is proposed and in addition to modeling and simulation, curve fitting is used to obtain the optimized modeling parameters. In Section 3 a description of the particle swarm optimization (PSO) and the values that are used to simulate the optimized PID parameters are presented. In Section 4 a description of the use of MATLAB in conjunction with the dSPACE hardware is given as well as an account of the development of a control platform. The experiments used to investigate the feasibility of the optimized PID control are also described, and Section 5 is the conclusion.

2. **Magnetic Bearing Modeling.** The electromagnetic levitation system with a single degree of freedom, used in this study, is a hybrid magnetic bearing, as shown in Figure 1. It has upper and lower hybrid bearings, a rotor and a base, and the construction is such that when the rotor reaches equilibrium a tiny air gap will remain between the bearings and rotor. The active magnetic bearing system has a servo control system of electromagnetic levitation actuators, controllers, position sensors and a linear power amplifier. The top and bottom bearings are connected in series by two sets of solenoid coils. A voltage V_{in} is input to the coil and the current generates a magnetic field. The strength of the current x_3 is related to the force acting on the rotor, and the total inductance will change along with the air gap (position) between the rotor and the top (up) and bottom (down) bearings.

According to Newton's second law of motion, the vertical position of the rotor can be represented by x_1, and speed by x_2. Therefore, the position and speed of movement are expressed in Equation (1), and the vertical movement of the rotor subject to the top and bottom bearing magnetic forces and the gravitational effect are expressed in Equation (2). A list of symbols used is given in Table 1.

$$\dot{x}_1 = x_2 \tag{1}$$

$$m\dot{x} = F_1 + F_2 - mg \tag{2}$$

Since the force terms F_1 and F_2 in the dynamic equation are affected by the air gap and the current input to the top and bottom bearings, the air gap and the current are variables for the measurement of the magnetic force applied to the rotor. The Matlab Surface Fitting Tool was used to fit the measurement data into quadratic polynomials, to

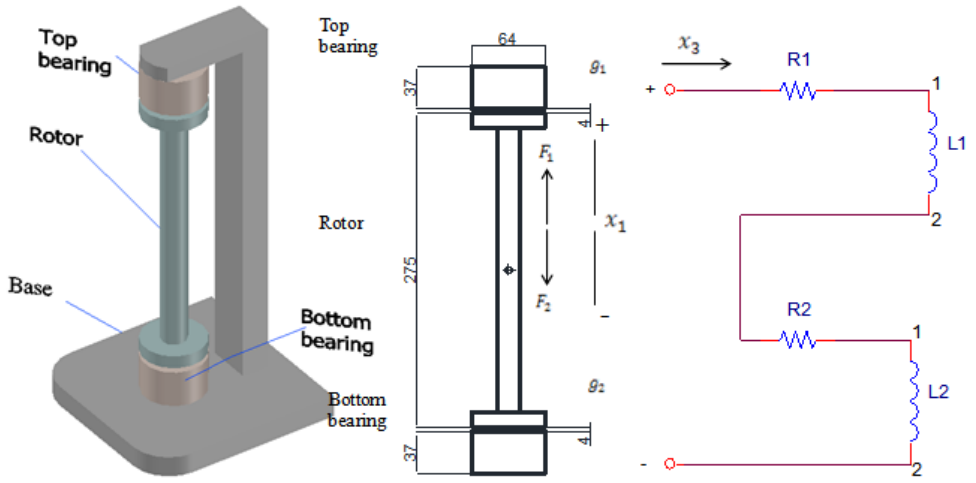

FIGURE 1. Magnetic bearing with a single degree of freedom

TABLE 1. Magnetic bearing system terminology

Symbol	**Definitions**	Units
x_1	Rotor position	Meter (m)
x_2	Rotor vertical speed	meters/second (m/s)
m	Rotor mass	Kilogram (kg)
F_1	Magnetic force at top bearing acting on rotor (upward)	Newton (N)
F_2	Magnetic force at bottom bearing acting on rotor (downward)	Newton (N)
g	Gravitational constant	(m/s^2)
g_1	Top bearing air gap	(mm)
g_2	Bottom bearing air gap	(mm)
x_3	Current	Ampere (A)
V_{in}	Voltage	volt (V)
R_T	Total resistance bearing series coil	Ohm (Ω)
L_T	Total inductance with mutual inductance of top and bottom bearing series coil	Henry (H)

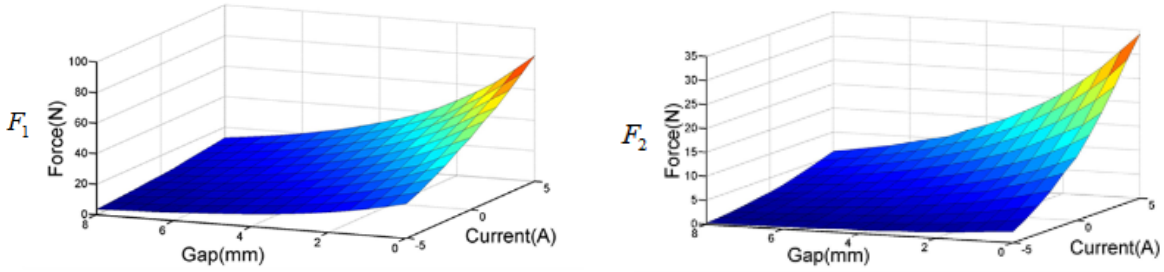

(a) (b)

FIGURE 2. Magnetic force applied by top and bottom bearings to the rotor

give Equations (3) and (4), and the curve fitting result is shown in Figure 2.

$$F_1 = g \cdot \left(4.807 + 0.5149 \cdot x_3 - 1.032 \cdot g_1 + 0.009643 \cdot x_3^2 - 0.06011 \cdot x_3 \cdot g_1 + 0.06677 \cdot g_1^2\right) \tag{3}$$

$$F_2 = g \cdot \left(1.439 + 0.278 \cdot x_3 - 0.3182 \cdot g_2 + 0.009844 \cdot x_3^2 - 0.03159 \cdot x_3 \cdot g_2 + 0.02036 \cdot g_2^2\right) \tag{4}$$

Based on the relationship between voltage and current as described by Kirchhoff's Laws, Equations (5) to (8) are obtained.

$$L_T \cdot \dot{x}_3 + R_T \cdot x_3 - V_{in} = 0 \tag{5}$$

$$\dot{x}_3 = \frac{V_{in} - R_T \cdot x_3}{L_T} \tag{6}$$

$$\text{Total resistance} \quad R_T = R_1 + R_2 \quad \text{unit } (\Omega) \tag{7}$$

$$\text{Total inductance} \quad L_T = L_1 + L_2 + L(x_1) \quad \text{unit (H)} \tag{8}$$

The total inductance L_T, not only takes the electromagnet inductance L_1 and L_2 of the top and bottom bearing into account, but also considers the mutual inductance $L(x_1)$ with the rotor. The mutual inductance $L(x_1)$ changes along with position x_1 and by measuring the relationship between the position and the total inductance can be fitted as expressed

by Equation (9). The fitting curve is shown in Figure 3.

$$L_T = -0.001 \cdot x_1^2 - 0.0199 \cdot x_1 + 11.684 \tag{9}$$

In addition, upwards is defined as positive, downwards as negative. In the middle the position is defined as $x_1 = 0$, and at this time, the top and bottom bearing air gaps are both 4mm. The conversions between position and air gap are expressed by Equations (10) and (11).

$$g_1 = (0.004 - x_1) \cdot 1000 \tag{10}$$

$$g_2 = (0.004 + x_1) \cdot 1000 \tag{11}$$

The magnetic state of the model magnetic bearing system can be fully expressed by a set of three coupled Equations (12), (13) and (14)

$$\dot{x}_1 = x_2 \tag{12}$$

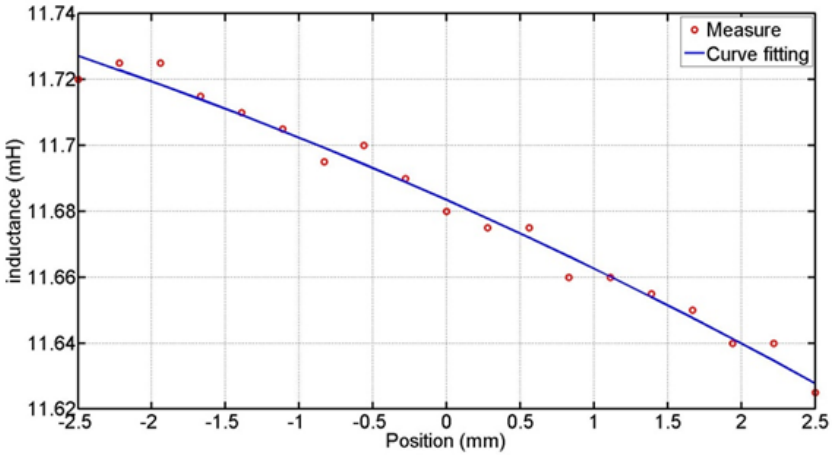

FIGURE 3. Curve fitting for position – total inductance

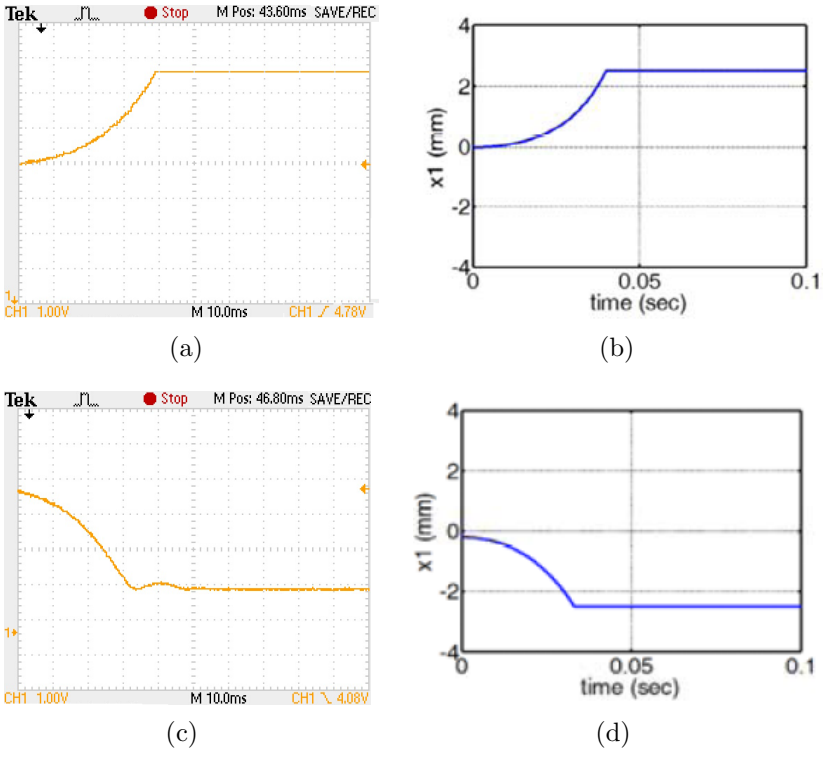

FIGURE 4. Magnetic bearing open system tests

$$m\dot{x}_2 = F_1 + F_2 - mg \tag{13}$$

$$\dot{x}_3 = \frac{V_{in} - R_T \cdot x_3}{L_T} \tag{14}$$

The experimental verification is shown in Figure 4. It shows that the experimental and simulation results are in very good agreement.

3. **Magnetic Bearing Control Simulation.** The PID controller architecture devised in this study is shown in Figure 5, wherein the fitness function uses the IAE (Integral-Absolute-Error) performance index for the fitness evaluation, and its definition is as follows:

$$J_{IAE} = \int_0^t \|e(t)\| dt \tag{15}$$

Figure 6(a) is the convergence curve simulation graph of the fitness function by PSO [7]. From the graph, it can be seen that after about 40 iterations, a stable state can be achieved and the optimizing PID control parameters are Kp = 38.68; Ki = 0.008; Kd = 0.51. The simulation result of the PID control is as shown in Figure 6(b). From the graph, it can be seen that the system can reach the stabilized equilibrium at position $x_1 = 0$ within 0.2 seconds.

4. **Result of the Magnetic Bearing Control Experiment.** The simulation results obtained in the previous section were used to achieve the control of an actual system. The control platform used was the control strategy package developed by dSPACE GmbH, Paderborn, Germany. The experimental system architecture was as shown in Figure 7(a). By substituting the optimizing PID control parameters of Kp = 39.5, Ki = 0.006, and

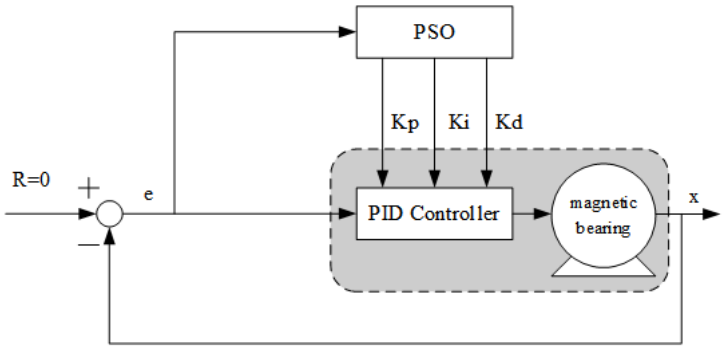

FIGURE 5. Control system architecture diagram

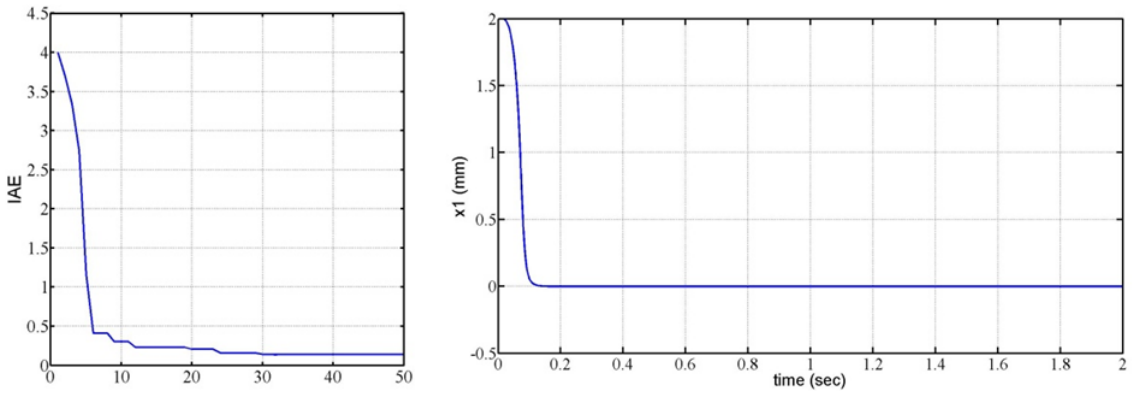

(a) (b)

FIGURE 6. PSO optimization process

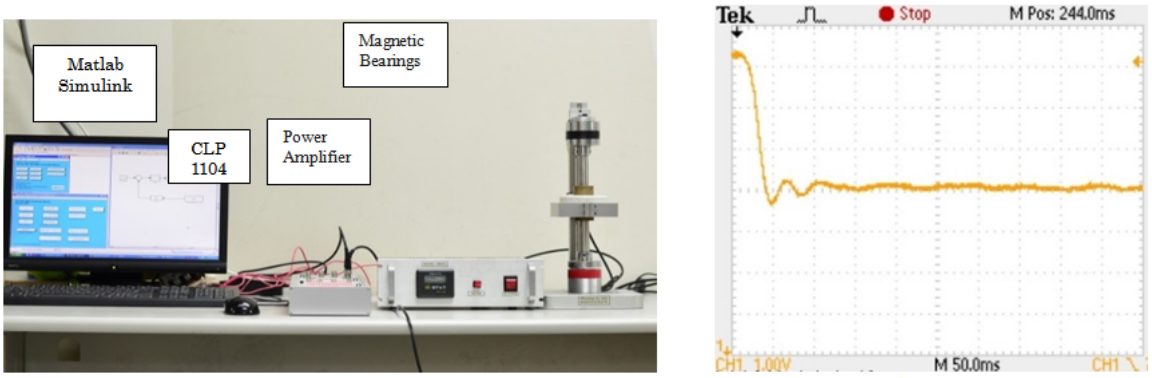

(a) (b)

FIGURE 7. Actual implementation of control platform system

Kd = 0.53 from the value simulation, the dynamic response of the bearing system obtained was found to be similar to the graph shown in Figure 7(b). The results of the experiment show that a magnetic bearing system can be stabilized to reach an equilibrium of $x_1 = 0$ in a short time, and the results also show that the control method proposed was feasible.

5. **Conclusion.** In this study a method for curve fitting was used to model a magnetic bearing system. Experiments were then conducted to verify that the modeling system dynamic equation was accurate and would completely describe an actual magnetic bearing system. In order to control the magnetic bearing system, the simplest PID control method was used in this study. The particle swarm optimization was applied to determine the PID control parameters and the optimal control parameters. Finally, experiments were conducted to verify the results and showed that the strategy proposed in the present research was feasible. Otherwise, the control law was achieved by PC based controller in this study. In the future, this control scheme could be implemented by microchip controller such as field-programmable array (FPGA). Therefore, the controller implement will be simpler and less expensive.

REFERENCES

[1] C. Toh and S. Chen, Development and experimental test of hybrid magnetic bearing for ring-type flywheel, *IEEE Magnetics Conference*, 2015.

[2] Y. D. Chung and C. Y. Lee, Feasible study of wireless power charging system for EDS-based superconducting magnetic levitation train using HTS receiver, *The 9th International Conference on Power Electronics and ECCE Asia*, pp.2328-2334, 2015.

[3] Y. Zhou, B. Kou, X. Yang and H. Zhang, Analysis and design of a low stiffness flat type vertical-gap passive maglev vibration isolation unit, *IEEE Magnetics Conference*, 2015.

[4] M. Lashin, A. T. Elgammal, A. Ramadan, A. A. Abouelsoud, S. F. M. Assal and A. Abo-Ismail, Fuzzy-based gain scheduling of exact feedforward linearization control and sliding mode control for magnetic ball levitation system: A comparative study, *IEEE International Conference on Automation, Quality and Testing, Robotics*, pp.1-6, 2014.

[5] D. Moreno, Design and implementation of an uncoupled and parallelly actuated control for the highly nonlinear suspension system of a maglev train, *The 6th International Conference on Intelligent Systems, Modelling and Simulation*, pp.199-204, 2015.

[6] M. Y. Chen, T. B. Lin, S. K. Hung and L. C. Fu, Design and experiment of a macro-micro planar maglev positioning system, *IEEE Trans. Industrial Electronics*, vol.59, pp.4128-4139, 2012.

[7] R. J. Rajesh and C. M. Ananda, PSO tuned PID controller for controlling camera position in UAV using 2-axis gimbal, *International Conference on Power and Advanced Control Engineering*, pp.128-133, 2015.